**7.12**

a) Determine an expression that gives the heat flow $Q$ (W) through a solid spherical shell with inside and outside radii of $r_1$ and $r_2$, respectively.

b) Examine the results regarding what happens as the shell thickness becomes larger compared with the inside radius.

**7.13** A sphere of radius $R$ is in a motionless fluid (no forced or natural convection). The surface temperature of the sphere is maintained at $T_R$ and the bulk fluid temperature is $T_\infty$. a) Develop an expression for the temperature in the fluid surrounding the sphere. b) Determine the Nusselt number for this situation. Such a value would be the limiting value for the actual system with convection as the forces causing convection become very small.

**7.14** For the system in Fig. 2.1 develop an expression for the temperature distribution in the falling film. Assume fully developed flow, constant properties, and fully developed temperature profile. The free liquid surface is maintained at $T = T_0$ and the solid surface at $T = T_s$, where $T_0$ and $T_s$ are constants. a) Ignore viscous heating effects. b) Include viscous heating effects.

*Answer b)*

$$\frac{T - T_0}{T_s - T_0} = \frac{x}{\delta}\left\{1 + \tfrac{3}{4}\,\mathrm{Br}\left[1 - \left(\frac{x}{\delta}\right)^3\right]\right\},$$

where $\mathrm{Br} = \dfrac{\eta \bar{V}^2}{k(T_s - T_0)}$, Brinkman number.

**7.15** Consider heat conduction through a plane wall of thickness $\Delta x$, and $T_1$ and $T_2$ are the surface temperatures. Derive the steady-state heat flux in terms of $T_1$, $T_2$ and $\Delta x$ if the thermal conductivity varies according to

$$k = k_0(1 + aT)$$

where $k_0$ and $a$ are constants.

**7.16** A liquid at a temperature $T_0$ continuously enters the bottom of a small tank, overflows into a tube, and then flows downward as a film on the inside. At some position down the tube ($z = 0$) when the flow is fully developed, the pipe heats the fluid with a uniform flux $q_R$. The heat loss from the liquid's surface is sufficiently small so that it may be neglected.

a) For steady-state laminar flow with constant properties, develop by shell balance or show by reducing an equation in Table 7.5 the pertinent differential energy equation that applies to the falling film.

b) Write the boundary conditions for the heat flow.

c) What other information must complement parts a) and b) in order to solve the energy equation?

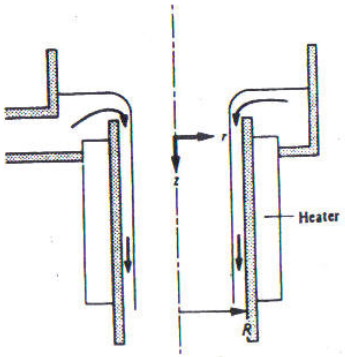




# 8

# CORRELATIONS AND DATA FOR HEAT TRANSFER COEFFICIENTS

The problems of heat flow with convection, discussed in the preceding chapter, pertain to simple systems with laminar flow. Despite the simplicity of laminar flow problems, they should not be underestimated. Many simple solutions have been applied to real systems with approximating assumptions and, besides, the simpler systems provide models for interpretation of complex systems. The more complex nature of turbulent flow and its limited accessibility to mathematical treatment requires, however, an empirical approach to heat transfer. On the other hand, the study of turbulent flow is not entirely empirical; it is possible to establish certain theoretical bases for the analyses of turbulent transfer processes and an introduction to this complex area is given in Chapter 16.

Figure 8.1 illustrates heat transfer in a bounded fluid. The fluid is artificially subdivided into three regions: the turbulent core, the transition zone, and the laminar sublayer near the surface. In the turbulent core, thermal energy is transferred rapidly due to the eddy (mixing) action of turbulent flow. Conversely, within the laminar sublayer, energy is transferred by conduction alone—a much slower process than the eddy process. In the transition zone, energy transport by both conduction and by eddies is appreciable. Hence, most of the total temperature drop between the fluid and the surface is across the laminar sublayer and the transition zone. Within the turbulent core, the temperature gradients are quite shallow.

In Chapter 3, it was convenient to define a friction factor to deal with momentum transport in fluids in contact with surfaces. Similarly, for energy transport between fluids and surfaces, it is convenient to define a heat transfer coefficient by

$$h = \frac{q_0}{T_0 - T_f} = \frac{-k(\partial T/\partial y)_0}{T_0 - T_f}, \tag{8.1}$$

where the subscript "0" refers to the respective quantities evaluated at the wall, and $T_f$ is some temperature of the fluid. If the fluid is infinite in extent, we take $T_f$ as the fluid temperature far removed from the surface, and designate it $T_\infty$. If the fluid flows in a confined space, such as inside a tube, $T_f$ is usually the *mixed mean temperature*, denoted by $T_m$; it is a temperature that would exist if the fluid at a particular cross section were removed and allowed to mix adiabatically.

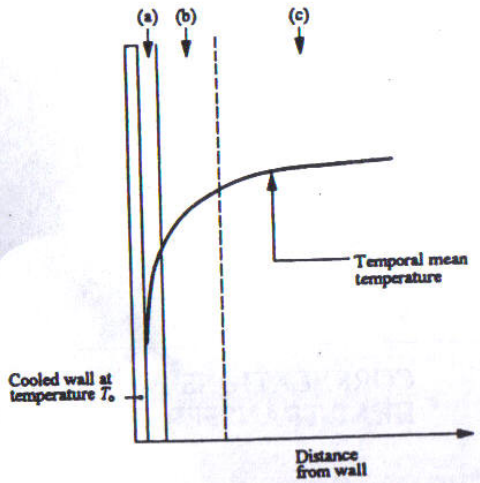


**Fig. 8.1** Temperature profile of a flowing fluid bounded by a cooler wall; (a) laminar sublayer, (b) transition zone, and (c) turbulent core.

As explained in Chapter 7, $h$ is a function of the fluid's properties ($k$, $\eta$, $\rho$, $C_p$), the system geometry, the flow velocity, and the value of the defining temperature difference. We deal in the remainder of this chapter with predicting the dependence of $h$ on these quantities, by presenting experimental data for various systems in the form of correlations based on dimensional analysis.

## 8.1 HEAT TRANSFER COEFFICIENTS FOR FORCED CONVECTION IN TUBES

In Section 3.1, we presented a method of dimensional analysis utilizing a rearrangement of differential equations in order to show that the friction factor was a function of the Reynolds number. We used the same method in Section 7.3 for natural convection. Here we bring the reader's attention to a different technique of dimensional analysis, while deriving those dimensionless numbers which are pertinent to the heat transfer system of forced convection within a tube.

### 8.1.1 Dimensional analysis—Buckingham's pi theorem

We may obtain pertinent dimensionless numbers without reference to the basic differential equations, if we can identify the variables sufficient to specify a given situation. A systematic way of determining the groups is known as *Buckingham's pi theorem*.[1] Simply stated, it reads: *The functional relationship among q quantities, whose units may be given in terms of u fundamental units, may be written as a function of q - u dimensionless groups (the π's).*

[1] E. Buckingham, *Trans. ASME* 35, 262 (1915).



In the application of the pi theorem, these rules are helpful:

a) Compile a list of the $q$ significant quantities and their respective fundamental units. The fundamental units are $L$ (length), $M$ (mass), $\Theta$ (time), and $T$ (temperature).

b) Select the primary quantities or primary $q$'s. The number of primary $q$'s should equal $u$, the number of fundamental units.

c) Form each $\pi$ term by expressing the ratio of the remaining $q$'s (one at a time) to the product of the primary $q$'s, each raised to an unknown power determined as shown below.

We now illustrate the method for heat transfer in forced convection. We presume that the heat transfer coefficient for fully developed forced convection in a tube is a function of the variables

$$h = f(\bar{V}, \rho, k, \eta, C_p, D). \tag{8.2}$$

We can express all these quantities in terms of the four fundamental dimensions $M$, $L$, $\Theta$, and $T$. Specifically,

| | | |
|---|---|---|
| $\bar{V}$, $L\Theta^{-1}$, | $\eta$, $ML^{-1}\Theta^{-1}$, | $D$, $L$. |
| $\rho$, $ML^{-3}$, | $C_p$, $L^2\Theta^{-2}T^{-1}$, | |
| $k$, $ML\Theta^{-3}T^{-1}$, | $h$, $M\Theta^{-3}T^{-1}$, | |

Note that energy is given the units of work (force × distance), namely, $ML^2\Theta^{-1}$.

The number of fundamental units in this case is four. Thus, since $u = 4$, select as the four primary $q$'s, $\bar{V}$, $D$, $\rho$, and $k$, leaving $h$, $\eta$, and $C_p$. Proceed to form the first $\pi$ term.

$$\pi_1 = \frac{h}{\bar{V}^a D^b \rho^c k^d} = \frac{M\Theta^{-3}T^{-1}}{(L\Theta^{-1})^a (L)^b (ML^{-3})^c (ML\Theta^{-3}T^{-1})^d}.$$

Equating the exponents of each dimension to zero, so that the $\pi$ group is dimensionless, we obtain

$$\begin{aligned} M&: \ 1 = c + d, \\ L&: \ 0 = a + b - 3c + d, \\ \Theta&: \ -3 = -a - 3d, \\ T&: \ -1 = -d. \end{aligned}$$

Solving these four equations simultaneously, we obtain $a = 0$, $b = -1$, $c = 0$, and $d = 1$. Thus

$$\pi_1 = \frac{hD}{k} \equiv \text{Nu} \qquad \text{(Nusselt number)}.$$

Similarly, the following $\pi$ groups can be obtained:

$$\pi_2 = \eta/\rho\bar{V}D \equiv \frac{1}{\text{Re}},$$

$$\pi_3 = C_p\eta/k \equiv \text{Pr} \qquad \text{(Prandtl number)}.$$

Thus, heat transfer data in forced convection can be correlated in terms of these three groups or dimensionless numbers:

$$\text{Nu} = \text{Nu}(\text{Re},\text{Pr}). \tag{8.3}$$

Equation (8.3) is not complete enough in some situations. If fully developed flow is not assumed, then the length to diameter ratio $L/D$ must be included. In addition, for large temperature differences, the temperature dependence of the fluid viscosity may be handled approximately by including the group $\eta_m/\eta_0$, where $\eta_m$ is the viscosity at the mixed mean temperature $T_m$, and $\eta_0$ is the viscosity at the temperature of the solid surface. Hence, a complete correlation is written in the form

$$\mathrm{Nu} = \mathrm{Nu}(\mathrm{Re}, \mathrm{Pr}, L/D, \eta_m/\eta_0). \tag{8.4}$$

This dimensional analysis is of great use in experimental work involving heat transfer. For example, $h$ depends on eight physical quantities: $D$, $\overline{V}$, $\rho$, $\eta_m$, $\eta_0$, $C_p$, $k$, and $L$. To study all combinations of eight independent variables for ten values of each would require $10^8$ tests, whereas, by giving Nu as a function of only four groups $(\mathrm{Re}, \mathrm{Pr}, L/D, \eta_m/\eta_0)$, $10^4$ tests would suffice. Thus, a graduate student would require only five years of research instead of 50,000 years!

### 8.1.2 Correlations for forced convection in tubes

For fully developed flow in tubes, a correlation for flow in smooth tubes with nearly constant wall temperature is presented in Fig. 8.2. The Reynolds number used here, $\mathrm{Re}_m = D\overline{V}\rho/\eta_m$, is convenient because the laminar-to-turbulent transition is at about 2100 (the same as in Fig. 3.2), even when $\eta_0$ differs appreciably from $\eta_m$.

For highly turbulent flow ($\mathrm{Re}_m > 10{,}000$), the equation

$$\mathrm{Nu}_m = 0.026\ \mathrm{Re}_m^{0.8}\ \mathrm{Pr}_m^{1/3} \left(\frac{\eta_m}{\eta_0}\right)^{0.14} \tag{8.5}$$

reproduces experimental data to within about ±20% in the range $10^4 < \mathrm{Re}_m < 10^5$, $0.6 < \mathrm{Pr} < 100$, and $L/D > 10$. As we discuss later, the data need not be restricted to the situations of constant wall temperature.

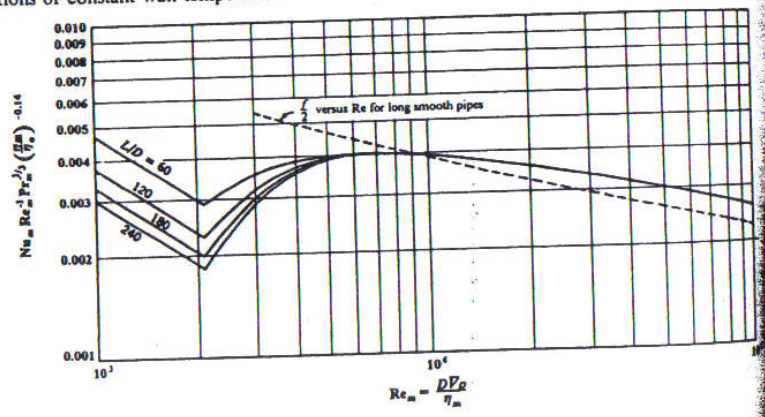


Fig. 8.2 Heat transfer coefficients for fully developed flow in smooth tubes. (From E. N. Seider and G. E. Tate, *Ind. Eng. Chem.* **28**, 1429 (1936).)



We superimpose the plot of $f/2$ on Fig. 8.2 for long, hydraulically smooth tubes, where

$$j_H = \mathrm{St}_m \left[\frac{C_{p,m}\eta_f}{k_m}\right]^{2/3} = \frac{f}{2}. \tag{8.6}$$

$\mathrm{St}_m$ is the Stanton number, and $j_H$ is often referred to as a *j-factor*. The Stanton number is defined

$$\mathrm{St} \equiv \frac{\mathrm{Nu}}{\mathrm{Re}\cdot\mathrm{Pr}} = \frac{h}{C_p\rho\overline{V}}.$$

Equation (8.6) is Colburn's analogy between heat transfer and fluid friction. The analogy breaks down for $\mathrm{Re}_m < 10{,}000$, and also for rough tubes because $f$ is affected more by roughness than its counterpart $j_H$. The effect of wall roughness was studied for air and Fig. 8.3 relates the heat transfer coefficient to the ratio of the friction factor $f$ in the rough pipe to the friction factor $f_s$ in a smooth pipe of the same diameter. The results have not been tested extensively, and should probably be restricted to use with gases.

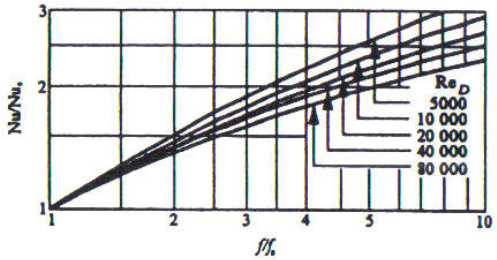


**Fig. 8.3** Effect of roughness on heat transfer in turbulent flow. (From W. Nunner, *VDI—Forschungsheft* No. 455/1956 (VID-Verlag GmbH-Dusseldorf).)

For liquid metals, where $0.005 < \mathrm{Pr} < 0.05$, the following equation represents available experimental data with $\mathrm{Re} > 10{,}000$ and for a uniform heat flux:[2]

$$\mathrm{Nu}_q = 6.7 + 0.0041(\mathrm{Re}\cdot\mathrm{Pr})^{0.793} \exp(41.8\ \mathrm{Pr}). \tag{8.7}$$

Because of the very high values of $h$ in liquid metals, $(T_0 - T_m)$ is not very large, so that the mixed mean temperature properties can be used without significant error.

Equation (8.7) for liquid metals applies to uniform heat flux along the tube. For uniform wall temperature, the difference between $\mathrm{Nu}_T$ (uniform wall temperature) and $\mathrm{Nu}_q$ (uniform heat flux) is significant for liquid metals (Fig. 8.4); for $\mathrm{Pr} > 0.5$ the difference between $\mathrm{Nu}_T$ and $\mathrm{Nu}_q$ is small, and hence Eq. (8.5) is also approximately valid for constant heat flux boundary conditions.

---

[2] W. M. Rohsenow and H. Y. Choi, *Heat, Mass, and Momentum Transfer*, Prentice-Hall, Englewood Cliffs, NJ, 1961, page 193.

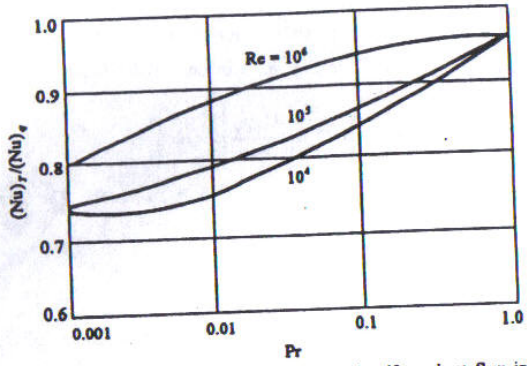


**Fig. 8.4** Comparison of uniform wall temperature and uniform heat flux in tubes. (From R. A. Seban and T. T. Shimazaki, *Trans. ASME* 73, 803 (1951).)

**Example 8.1** A 5 ton (4536 kg) heat of steel must be decarburized from 0.40 to 0.20% C in 5 min. A convenient method for accomplishing this is to blow oxygen through a submerged lance. A low carbon steel pipe of 12.7 mm I.D. is used as the lance, despite the fact that the end of the pipe gradually melts. If we estimate the portion of the lance within the furnace to be at 1744 K, calculate the temperature at which the oxygen enters the liquid steel. Neglect the pressure drop through the pipe and assume that the pressure in the pipe equals $1.22 \times 10^5$ N m$^{-2}$ (1.2 atm).

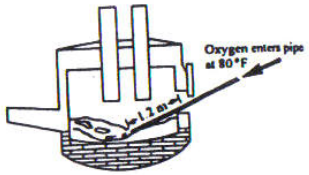


*Solution.* The oxygen requirement, for $C + \frac{1}{2}O_2(g) \rightarrow CO(g)$, is

$$\bar{V}\rho = \frac{(4536)(0.20)\text{ kg C}}{(100)(300)\text{ s}} \left| \frac{1\text{ kmol C}}{12.011\text{ kg C}} \right| \frac{0.5\text{ kmol O}_2}{1\text{ kmol C}} \left| \frac{32\text{ kg O}_2}{1\text{ kmol O}_2} \right| \frac{4}{\pi(12.7^2)\text{ mm}^2} \left| \frac{1000^2\text{ mm}^2}{1\text{ m}^2} \right.$$

$$= 318 \text{ kg m}^{-2} \text{ s}^{-1}.$$

The oxygen enters the tube at 300 K, and as it proceeds through the pipe its temperature rises. Consequently, the properties of the oxygen vary with distance down the tube. A commonly employed estimation is to evaluate the properties of the fluid at its average temperature along the heated pipe. The heat transfer coefficient corresponding to these properties is then calculated, assumed to be constant along the pipe, and used to determine the heat transferred to the gas.

First, arbitrarily assume that the gas leaves the pipe at 820 K. Then take the average $T_m$ as (820 + 300)/2 = 560 K for the last 1.2 m of pipe. At 560 K, the properties of $O_2$ are $\eta = 32.4 \times 10^{-6}$ kg m$^{-1}$ s$^{-1}$; $k = 45.8 \times 10^{-3}$ W m$^{-1}$ K$^{-1}$; $C_p = 991$ J kg$^{-1}$ K$^{-1}$; Pr = 0.701.



At 300 K, $\eta = 41.5 \times 10^{-6}$ kg m$^{-1}$ s$^{-1}$, which we use for $\eta_0$. Now calculate $Re_m$:

$$Re_m = \frac{D\bar{V}\rho}{\eta_m} = \frac{(12.7 \times 10^{-3})(318)}{(32.4 \times 10^{-6})} = 1.25 \times 10^5.$$

Then Eq. (8.5) applies, so that

$$Nu_m = 0.026\, Re_m^{0.8}\, Pr_m^{1/3} \left[\frac{\eta_m}{\eta_0}\right]^{0.14} = (0.026)(1.25 \times 10^5)^{0.8}(0.701)^{1/3}\left[\frac{32.4 \times 10^{-6}}{41.5 \times 10^{-6}}\right]^{0.14}$$

$$= 267.$$

Therefore

$$h = \frac{k_m Nu_m}{D} = \frac{(45.8 \times 10^{-3})(267)}{12.7 \times 10^{-3}} = 963 \text{ W m}^{-2} \text{ K}^{-1}.$$

An energy balance applied to the fluid over a differential length of pipe, $dx$, can be written

$$WC_p dT_m = h(T_0 - T_m)(\pi D dx),$$

where $W$ = mass flow rate, kg s$^{-1}$, and $T_0$ = temperature of pipe wall. Integrating for a length of pipe $L$, with $h$, $C_p$, and $T_0$ taken as constants, yields

$$h\int_0^L dx = -\frac{WC_p}{\pi D}\int_{\Delta T_L}^{\Delta T_0} d\ln(T_m - T_0),$$

or

$$\ln\frac{\Delta T_L}{\Delta T_0} = -\frac{hL\pi D}{WC_p} = -\frac{4hL}{\bar{\rho}\bar{V}C_p D}.$$

Substituting numerical values yields

$$\ln\frac{\Delta T_L}{(820 - 300)} = -\frac{(4)(963)(1.2)}{(318)(991)(12.7 \times 10^{-3})},$$

from which

$$\Delta T_L = 164 \text{ K} \quad \text{or} \quad T_m = 984 \text{ K (at } x = L = 1.2 \text{ m}).$$

Retaining our initial guess of 820 K, we see that in terms of estimating properties we have obtained reasonably good values.

As a second guess, assume that the gas leaves the pipe is 940 K. Then, we take the average $T_m$ as (940 + 300)/2 = 620 K. At 620 K, the properties of $O_2$ are $\eta = 35.1 \times 10^{-6}$ kg m$^{-1}$ s$^{-1}$; $k = 48.4 \times 10^{-3}$ W m$^{-1}$ K$^{-1}$; $C_p = 1010$ J kg$^{-1}$ K$^{-1}$; Pr = 0.732.

When we repeat the method of calculation using these new values, we get $Re_m = 1.15 \times 10^5$, $Nu_m = 256$, and $h = 976$ W m$^{-2}$ K$^{-1}$. The difference between the first and the second estimates of $h$ is only 1.3%. Finally, $\Delta T_L = 165$ K, or $T_m = 985$ K (at $x = L = 1.2$ m). We could repeat the process, but of course our second result is practically the same as the first. Hence, it is not necessary to do so.

The conclusion that the gas temperature is lower than the metal temperature when it exits from the lance becomes significant when the bubble size is calculated in order to obtain the surface area and residence time for calculations of mass transfer. Since the gas is not fully expanded when it exits from the pipe, the bubble size, calculated on the basis of the pipe size, is smaller than the ultimately expanded bubble size, and the rate of rise is faster than anticipated on the basis of the pipe size.

## 8.2 HEAT TRANSFER COEFFICIENTS FOR FORCED CONVECTION PAST SUBMERGED OBJECTS

In the following correlations, the heat transfer coefficient $h$ is defined for the total surface area of the submerged object, and the defining fluid temperature is that far removed from the surface. We evaluate all the properties, however, at the *film temperature*, $T_f = (T_0 + T_\infty)/2$.

In Fig. 8.5, $j_H = \mathrm{Nu}_f \mathrm{Re}_f^{-1} \mathrm{Pr}_f^{1/3}$ is plotted versus Re for a long cylinder perpendicular to the fluid. The figure also shows a plot of $f/2$ versus Re to illustrate that $j_H < f/2$, which is usually the case in flows with curved streamlines. Colburn's analogy breaks down here because of the form drag which has no counterpart in heat transfer.

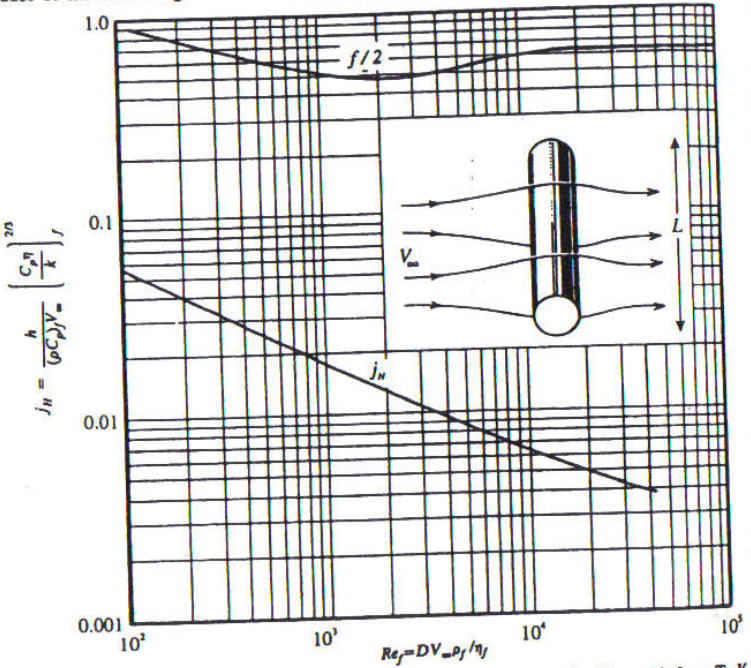


**Fig. 8.5** Heat and momentum transfer for a cylinder perpendicularly oriented to flow. ($j_H$ from T. K. Sherwood and R. L. Pigford, *Absorption and Extraction*, second edition, McGraw-Hill, New York, 1952, page 70; $f$ from F. Eisner, see Fig. 3.9.)



These results agree closely with McAdams' correlation[3] which is based on experiments with water, oils, and air. Over the range $1 < \mathrm{Re}_f < 10^3$, McAdams specifies

$$\mathrm{Nu}_f \mathrm{Pr}_f^{-0.3} = 0.35 + 56\ \mathrm{Re}_f^{0.52}. \tag{8.8}$$

For higher Reynolds numbers, $10^3 < \mathrm{Re} < 5 \times 10^4$, data collected for air are correlated by

$$\mathrm{Nu}_f \mathrm{Pr}_f^{-0.3} = 0.26\ \mathrm{Re}_f^{0.60}. \tag{8.9}$$

More recent correlations are summarized by Holman,[4] among which the most comprehensive is that given by Churchill and Bernstein:[5]

$$\mathrm{Nu}_f = 0.3 + \frac{0.62\ \mathrm{Re}_f^{1/2}\ \mathrm{Pr}_f^{1/3}}{\left[1 + (0.4/\mathrm{Pr}_f)^{2/3}\right]^{3/4}} \left[1 + \left[\frac{\mathrm{Re}_f}{2.82 \times 10^5}\right]^{5/8}\right]^{4/5} \tag{8.10}$$

for $10^2 < \mathrm{Re}_f < 10^7$ and $\mathrm{Re}_f \mathrm{Pr}_f > 0.2$. Equation (8.10) was tested against data for air, water, and liquid sodium so it has a wide range of applicability. Notice, however, that it is not useful for very small Reynolds numbers ($\mathrm{Re}_f < 100$); furthermore it underestimates data somewhat in the range $2 \times 10^4 < \mathrm{Re}_f < 4 \times 10^5$. For this range, the second brackets on the right-hand-side of Eq. (8.10) should be replaced with

$$1 + \left[\frac{\mathrm{Re}_f}{2.82 \times 10^5}\right]^{1/2}.$$

Holman[4] also gives correlations, based on empirical data, for heat transfer between fluids and noncircular cylinders.

Figure 8.6 gives $\mathrm{Nu}_f$ for the flow past a sphere. The relationship plotted is

$$hD/k_f = 2.0 + 0.60(DV_\infty\rho_f/\eta_f)^{1/2}(C_p\eta/k)_f^{1/3}. \tag{8.11}$$

This equation predicts that Nu approaches 2 as Re approaches zero; we can calculate this result for pure conduction, from a sphere at a uniform temperature in an infinite stagnant medium. Another correlation for heat transfer between fluids and spheres is that given by Whitaker:[6]

$$\mathrm{Nu}_\infty = 2 + \left(0.4\ \mathrm{Re}_\infty^{1/2} + 0.06\ \mathrm{Re}_\infty^{2/3}\right) \mathrm{Pr}_\infty^{0.4} \left[\frac{\eta_\infty}{\eta_s}\right]^{1/4}, \tag{8.12}$$

where the properties are evaluated at the temperature of the free stream, except $\eta_s$, which is the viscosity at the temperature of the sphere. The ranges for Eq. (8.12) are $0.71 < \mathrm{Pr}_\infty < 380$, $3.5 < \mathrm{Re}_\infty < 7.6 \times 10^4$, and $1.0 < (\eta_\infty/\eta_s) < 3.2$. Neither Eq. (8.11) nor (8.12) should be used for liquid metals.

---

[3] W. H. McAdams, *Heat Transmission*, third edition, McGraw-Hill, New York, 1954, page 268.

[4] J. P. Holman, *Heat Transfer*, sixth edition, McGraw-Hill, New York, 1986, pages 292-296.

[5] S. W. Churchill and M. Bernstein, *J. Heat Transfer* **99**, 300 (1977).

[6] S. Whitaker, *AIChE J.* **18**, 361 (1972).

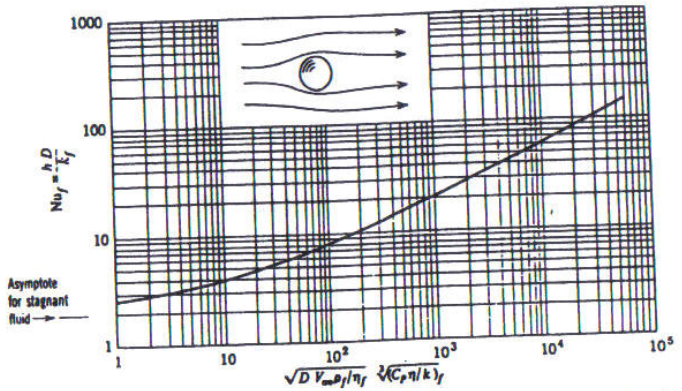


**Fig. 8.6** Heat transfer from a sphere to a flowing fluid. (From W. E. Ranz and W. R. Marshall, Jr., *Chem. Eng. Prog.* **48**, 141-146, 173-180 (1952).)

Figure 8.7 shows results for the flow parallel to an isothermal semi-infinite flat plate. For this flow system, the Colburn analogy holds very well because there is no form drag; therefore, the local heat transfer coefficient is related to the friction factor by

$$\frac{h_x}{C_p \rho V_\infty} \mathrm{Pr}^{2/3} = \frac{f_x}{2}. \tag{8.13}$$

For turbulent flow (from Fig. 3.5), $f_x = 0.0592\ \mathrm{Re}_x^{-1/5}$; then Eq. (8.13) is

$$\frac{h_x}{C_p \rho V_\infty} \mathrm{Pr}^{2/3} = 0.0296\ \mathrm{Re}_x^{-1/5}, \tag{8.14}$$

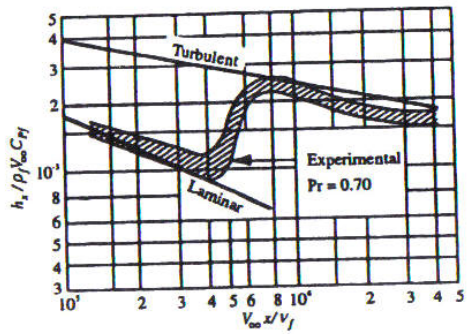


**Fig. 8.7** Heat transfer coefficient for flow over flat plate with turbulent boundary layer and uniform heat flux. Experimental data collected for air, and compared to the analysis for turbulent flow (Eq. (8.12)), and laminar flow (Eq. (7.27)). (From R. A. Seban and D. L. Doughty, *Trans. ASME* **78**, 217 (1956).)



or

$$\frac{h_x x}{k} = \mathrm{Nu}_x = 0.0296\ \mathrm{Re}^{0.8}\ \mathrm{Pr}^{1/3}. \tag{8.15}$$

The average coefficient $h$ between $x = 0$ and $x = L$ is

$$hL/k = \mathrm{Nu}_L = 0.037\ \mathrm{Re}_L^{0.8}\ \mathrm{Pr}^{1/3}. \tag{8.16}$$

(Here the initial part of the plate where laminar flow could exist has been ignored.)

Equation (8.15) overestimates the experimental data by approximately 4 to 19 pct. The agreement can be improved simply by modifying Eq. (8.15), so it becomes

$$\mathrm{Nu}_x = 0.026\ \mathrm{Re}^{0.8}\ \mathrm{Pr}^{1/3}. \tag{8.17}$$

The data agree with the laminar boundary layer result (Eq. (7.27)). Note that Eqs. (8.13)-(8.17) are valid for $\mathrm{Pr} > 0.5$, but not for liquid metals; the equations are valid for either uniform wall temperature or uniform heat flux.

**Example 8.2** A hot-wire anemometer is a device which indirectly measures the velocity of a moving fluid. It is usually a platinum wire which is heated electrically and positioned normal to the motion of the fluid. At a steady power input to the wire, its temperature reaches a steady value which can be related to the fluid velocity. The temperature of the wire is determined by measuring current, voltage drop, and hence electrical resistance, and by knowing how the resistance varies with the temperature. Thus, both the heat flux—from the wire to the fluid—and the wire temperature are measured electrically. Given air at 290 K flowing normal to the wire (3 mm in diameter) at 330 K, with a heat flux of 6300 W m$^{-2}$, determine the velocity of the air.

*Solution.* Assume that Eq. (8.9) applies:

$$\mathrm{Nu}_f\ \mathrm{Pr}_f^{-0.3} = 0.26\ \mathrm{Re}_f^{0.60},$$

$$h = \frac{q_0}{\Delta T} = \frac{6300}{(330 - 290)} = 157.5\ \mathrm{W\ m^{-2}\ K^{-1}}.$$

Use the properties of air at $T_f = 310$ K: $\rho = 1.13$ kg m$^{-3}$; $C_p = 1.01 \times 10^3$ J kg$^{-1}$ K$^{-1}$; $k = 27.0 \times 10^{-3}$ W m$^{-1}$ K$^{-1}$; $\eta = 1.89 \times 10^{-5}$ kg m$^{-1}$ s$^{-1}$; $\mathrm{Pr}_f = 0.705$.

$$\mathrm{Nu}_f = \frac{hD}{k_f} = \frac{(157.5)(0.003)}{(27.0 \times 10^{-3})} = 17.5,$$

$$\mathrm{Re}_f^{0.60} = \frac{(17.5)}{(0.705)^{0.3}(0.26)} = 74.75,$$

$$\mathrm{Re}_f = 1326.$$

Thus, Eq. (8.9) applies as assumed, and

$$V_\infty = \left[\frac{\eta_f}{\rho_f}\right]\left[\frac{\mathrm{Re}_f}{D}\right] = \left[\frac{1.89 \times 10^{-5}}{1.13}\right]\left[\frac{1326}{0.003}\right] = 7.40\ \mathrm{m\ s^{-1}}.$$

## 8.3 HEAT TRANSFER COEFFICIENTS FOR NATURAL CONVECTION

In Chapter 7, the discussion of natural convection in laminar flow led to a dimensionless equation of the form

$$\mathrm{Nu} = \mathrm{Nu}(\mathrm{Gr},\mathrm{Pr}).$$

This corresponds to the results of dimensional analysis in this chapter if the Reynolds number, the important number for forced convection, is replaced by the Grashof number, the important number for natural convection.

Figure 8.8 shows the results of correlating experimental data for free convection from vertical plates and horizontal cylinders to gases and liquids with Prandtl numbers ranging from about 0.5 to 10. The effect of the variation of properties with temperature is included by evaluating properties at $T_f = \frac{1}{2}(T_0 + T_\infty)$. The dimensionless numbers are then defined as $\mathrm{Nu}_L \equiv \dfrac{hL}{k_f}$, $\mathrm{Pr} \equiv \dfrac{\nu_f}{\alpha_f} = \dfrac{C_p\eta_f}{k_f}$, and $\mathrm{Gr}_L \equiv g\,\dfrac{L^3\rho_f^2\beta_f(T_0 - T_\infty)}{\eta_f^2}$.

The characteristic dimension $L$ is the plate length. For cylinders, the characteristic dimension is one-half the circumference, that is, $\pi D/2$; by defining $L$ as such, note how closely the curves for the two different correlations lie. In fact, very often no distinction is made between these two cases, and a third case, namely, that of vertical cylinders with characteristic dimension taken as length, is included in the correlations.*

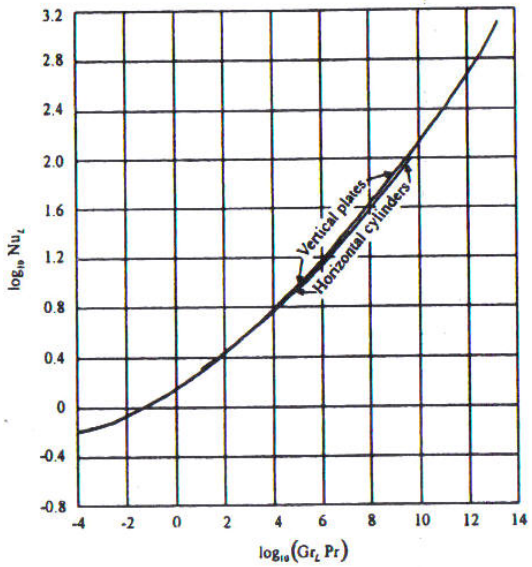


**Fig. 8.8** Heat transfer coefficients for natural convection. (From W. H. McAdams, *ibid.*, pages 173-176.)

*This procedure can be followed when $(D/L) \geq 35/(\mathrm{Gr}_L^{1/4})$ and $L$ is vertical length.



In Chapter 7, Ostrach's analysis of laminar natural convection past vertical plates led to Eq. (7.45). This relationship holds in the laminar flow region $10^4 < \mathrm{Gr}\,\mathrm{Pr} < 10^9$ for a wide range of Prandtl numbers ($0.00835 \leq \mathrm{Pr} \leq 1000$). For the sake of completeness, let us repeat it:

$$\frac{\mathrm{Nu}_L}{\sqrt[4]{\mathrm{Gr}_L/4}} = \frac{0.902\ \mathrm{Pr}^{1/2}}{(0.861 + \mathrm{Pr})^{1/4}}. \tag{7.45}$$

In the range of $0.6 < \mathrm{Pr} < 10$, the data can be represented by a much simpler equation (still for laminar flow):*

$$\mathrm{Nu}_L = 0.56(\mathrm{Gr}_L\,\mathrm{Pr})^{1/4}. \tag{8.18}$$

For liquid metals, the data in the laminar range for horizontal cylinders were correlated by[7]

$$\mathrm{Nu}_D = 0.53\left[\frac{\mathrm{Pr}}{0.952 + \mathrm{Pr}}\right]^{1/4}(\mathrm{Gr}_D\,\mathrm{Pr})^{1/4}. \tag{8.19}$$

The expression is of the same form as Eq. (7.45), and also closely corresponds numerically if the characteristic dimension $D$ (diameter) is replaced by $L$ taken as $\pi D/2$.

In the turbulent range of $10^9 < \mathrm{Gr}\,\mathrm{Pr} < 10^{12}$, the following equation has been proposed as possibly valid for a wide range of Pr for vertical plates[8] and horizontal cylinders with $L$ replaced by $\pi D/2$:

$$\mathrm{Nu}_L = 0.0246\ \mathrm{Gr}_L^{2/5}\ \mathrm{Pr}^{7/15}\left(1 + 0.494\ \mathrm{Pr}^{2/3}\right)^{-2/5}. \tag{8.20}$$

We use a much simpler form of Eq. (8.20) for $0.6 < \mathrm{Pr} < 10$:

$$\mathrm{Nu}_L = 0.13\ (\mathrm{Gr}_L\,\mathrm{Pr})^{1/3}. \tag{8.21}$$

Perhaps the most encompassing correlation for natural convection heat transfer from long horizontal cylinders is that of Churchill and Chu[9]; it is

$$\mathrm{Nu}_D = \left\{0.60 + \frac{0.387\,(\mathrm{Gr}_D\,\mathrm{Pr})^{1/6}}{\left[1 + (0.559/\mathrm{Pr})^{9/16}\right]^{8/27}}\right\}^2, \tag{8.22}$$

which applies for $10^{-5} < \mathrm{Gr}_D\,\mathrm{Pr} < 10^{12}$. In situations involving natural convection and mixed convection (forced convection plus natural convection) from very small diameter (<0.01 mm) cylinders, the results of Gebhart *et al.*[10] can be consulted.

*To make a distinction between plates and cylinders in Fig. 8.8, the coefficient 0.56 in Eq. (8.18) should be replaced by 0.59 and 0.53, respectively.

[7] *Reactor Handbook* 2; *Engineering*, AECD-3646 (May, 1955), page 283.

[8] W. M. Rohsenow and H. Y. Choi, *ibid.*, page 204.

[9] S. W. Churchill and H. H. S. Chu, *Int. J. Heat Mass Transfer* **18**, 1049 (1975).

[10] B. Gebhart, T. Andunson and L. Pera, in *Heat Transfer 1970*, U. Grigull and E. Hahne (editors), Elsevier Publishing, Amsterdam, 1970, Session NC3.2.

For a single *sphere* of diameter $D$ in a body of fluid, the relationship

$$\mathrm{Nu}_D = 2 + 0.060\ \mathrm{Gr}_D^{1/4}\ \mathrm{Pr}^{1/3}. \tag{8.23}$$

agrees with available data for $\mathrm{Gr}_D^{1/4}\ \mathrm{Pr}^{1/3} < 200$. In most instances, if the fluid is a gas, this restriction means that the equation applies to small particles. Note that the relationship yields $\mathrm{Nu}_D = 2$ when the fluid is motionless, as in Problem 7.14 where free convection is neglected.

Churchill[11] gives the following correlation for spheres in fluids with $\mathrm{Pr} \geq 0.7$ and $\mathrm{Gr}_D\ \mathrm{Pr} \leq 10^{11}$:

$$\mathrm{Nu}_D = 2 + \frac{0.589\ \mathrm{Gr}_D^{1/4}\ \mathrm{Pr}^{1/4}}{\left[1 + (0.469/\mathrm{Pr})^{9/16}\right]^{4/9}}. \tag{8.24}$$

**Example 8.3** Write an expression to relate the growth rate of a single spherical nucleus of solid as it develops in a pure supercooled liquid. Express the result in terms of $dR/dt$ as a function of supercooling $\Delta T$ and the properties of the metal. The thermal profile is depicted below; the temperature of the solid may be assumed as the freezing point $T_M$.

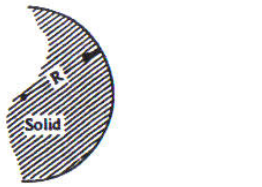


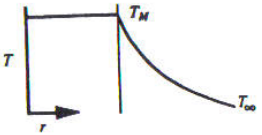


*Solution.* The rate at which latent heat of fusion evolves is equal to the rate at which heat flows from the interface into the bulk liquid

$$4\pi\rho_s H_f R^2 \frac{dR}{dt} = 4\pi R^2 h \Delta T,$$

where $\rho_s$ = density of the solid, $H_f$ = latent heat of fusion, and $\Delta T = T_M - T_\infty$ = amount of undercooling;

$$\frac{dR}{dt} = \frac{h}{\rho_s H_f}\Delta T.$$

From Eq. (8.23),

$$\frac{hD}{k} = 2 + 0.060\left[\frac{D^3\rho^2 g\beta\Delta T}{\eta^2}\right]^{1/4}\left[\frac{\eta C_p}{k}\right]^{1/3}.$$

When this is substituted into the expression for $dR/dt$, we obtain

$$\frac{dR}{dt} = \frac{k\Delta T}{\rho_s H_f}\left[\frac{1}{R} + 0.0504\left[\frac{\rho^2 g\beta\Delta T}{R\eta^2}\right]^{1/4}\left[\frac{\eta C_p}{k}\right]^{1/3}\right].$$

[11] S. W. Churchill, "Free Convection Around Immersed Bodies," in E. U. Schlünder, Ed.-in-Chief, *Heat Exchanger Design Handbook*, Section 2.5.7, Hemisphere Publishing Corp., New York, 1983.



Students of phase transformations are invited to use this as a basis for further discussion and/or refinement.

In the previous discussion of this section, heat transfer took place in the presence of convection mostly in the vertical direction. The convection behavior in the vicinity of horizontal surfaces is quite different, as shown in Fig. 8.9, and the correlations of Eqs. (8.18)-(8.21) do not apply. McAdams[12] recommends the following equations for some situations of natural convection from *horizontal* surfaces:

1. For a square plate with a surface warmer than the fluid facing upward, or cooler surface facing downward:

$$\mathrm{Nu}_L = 0.14(\mathrm{Gr}_L\ \mathrm{Pr})^{1/3}, \tag{8.25}$$

in the turbulent range, $2 \times 10^7 < \mathrm{Gr}_L < 3 \times 10^{10}$; and

$$\mathrm{Nu}_L = 0.54(\mathrm{Gr}_L\ \mathrm{Pr})^{1/4}, \tag{8.26}$$

in the laminar range, $10^5 < \mathrm{Gr}_L < 2 \times 10^7$.

2. For a square plate with a surface warmer than the fluid and facing downward, or cooler surface facing upward:

$$\mathrm{Nu}_L = 0.27(\mathrm{Gr}_L\ \mathrm{Pr})^{1/4}, \tag{8.27}$$

for $10^6 < \mathrm{Gr}_L\ \mathrm{Pr} < 10^{11}$.

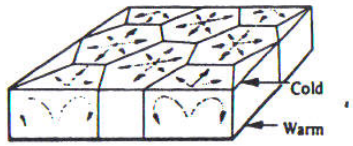


**Fig. 8.9** The convection pattern over a horizontal surface which is warmer than the fluid.

In Eqs. (8.25)-(8.27), $L$ is the length of the side of the square. As approximations, we can also apply the equations to horizontal circular disks with $L$ defined as 0.9 $D$ ($D$ being the disk diameter). The characteristic length, for a surface other than a square or a circle, should be taken as $L = A/P$ where $A$ is the surface area and $P$ is the perimeter.

In this very brief exposition of correlations used to estimate heat transfer coefficients, we have omitted many different geometrical and flow configurations. We recommend that

[12] W. H. McAdams, *ibid.*, page 180.

interested readers consult heat transfer texts, such as Holman,[13] Incropera and DeWitt,[14] Azbel,[15] and Karlekar and Desmond.[16]

## 8.4 QUENCHING HEAT TRANSFER COEFFICIENTS

In the next chapter, we present analytical expressions which describe the temperature during heating or cooling as a function of time and position within a solid. The most difficult variable to ascribe to such unsteady-state situations is probably the heat transfer coefficient governing the energy transport between the solid's surface and the surroundings. The methods of estimating $h$ for some convection systems, which were presented in previous sections of this chapter, can be applied satisfactorily to certain problems of unsteady-state heat flow. For the most part, however, correlations of $h$-values applicable to quenching operations have not been obtained because of the complexity of the convection systems.

Despite the importance of quenching operations in the heat treatment of alloys, materials engineers have not considered nearly enough of the quantitative aspects of quenching heat transfer, which is strongly linked to boiling heat transfer. Historically, the primary purpose of boiling heat transfer has been simply the conversion of liquid into vapor, and perhaps this is the reason why it has not been studied enough by materials engineers. On the other hand, engineers who are involved with the development of nuclear reactors, rocket nozzles, and spacecraft have conducted considerable research into the boiling process.

Although boiling is a familiar phenomenon, from the point of view of energy transport it is a complicated process. Figure 8.10 illustrates the complexities of boiling in which several regimes exist. If a heated metal surface is submerged in a pool of liquid at its saturation temperature, $T_{sat}$, the following events take place. As the surface temperature $T_w$ is raised above $T_{sat}$, convection currents circulate within the superheated liquid. Heat transfer with convection takes place, and the correlations discussed for natural convection in Section 8.3 apply. However, the liquid cannot be indefinitely superheated so that further increases of $(T_w - T_{sat})$ above approximately 2 K are accompanied by vapor bubbles forming at preferred sites on the surface. This is regime II, in which most of the bubbles do not exceed a certain size necessary for their escape. In regime III, $(T_w - T_{sat})$ is large enough so that larger and more stable bubbles grow, and at the same time more bubbles form because more nucleation sites become active on the solid's surface. This mechanism, which is called nucleate boiling, can generate very high heat fluxes. As the bubbles rapidly form and detach themselves from the surface, fresh liquid rushes to the former bubble site, and the very rapid process of bubble formation and detachment repeats itself over and over again. The net result is that all the bubble sites act as micropumps and create a large degree of convection at the surface.

If $(T_w - T_{sat})$ is raised to even higher values, for example, 40 K in water, then the nucleation sites on the surface become so numerous that the bubbles coalesce, and tend to

[13] J. P. Holman, *ibid.*, Chapters 6 and 7.

[14] F. P. Incropera and D. P. DeWitt, *Fundamentals of Heat and Mass Transfer*, third edition, John Wiley, New York, NY, Chapters 7, 8, and 9, 1990.

[15] D. Azbel, *Fundamentals of Heat Transfer for Process Engineering*, Noyes Publications, Park Ridge, NJ, Chapter 3, 1984.

[16] B. V. Karlekar and R. M. Desmond, *Engineering Heat Transfer*, West Publishing, St. Paul, MN, Chapters 8 and 9, 1977.



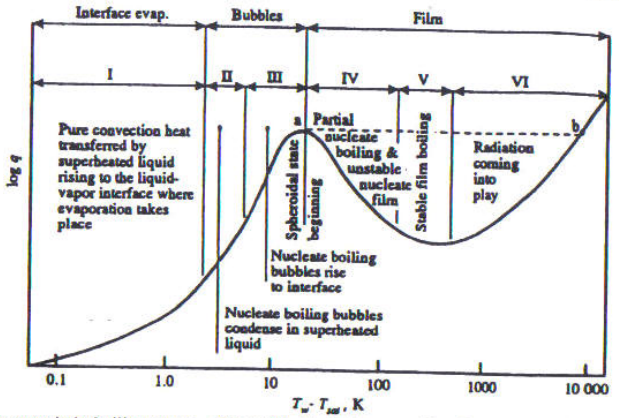


**Fig. 8.10** Characteristic boiling curve. (From W. M. Rohsenow, *Developments in Heat Transfer*, MIT Press, Cambridge, MA, 1964, Chapter 8.)

form a vapor blanketing layer. Beyond this point, the heat flux decreases with increasing$(T_w - T_{sat})$ because of the vapor's insulating nature.* Regime IV encompasses this effect wherein an unstable vapor film forms but collapses and reforms rapidly. For values of $(T_w - T_{sat})$ greater than about 480 K (for water), a stable film exists (regime V). This is called *film boiling*, with which rather low heat fluxes are associated (contrasted to nucleate boiling); for values of $(T_w - T_{sat})$ greater than 920 K, radiation across the vapor blanket becomes important, and the rate of heat transfer increases accordingly.

Returning to quenching, we see that Fig. 8.11 shows a typical cooling curve of a metal part plunged into water. Note the three distinct stages during the cooling process. Stage *A*, called the vapor cooling stage, occurs immediately upon immersing the part in the water. Liquid vaporizes adjacent to the surface and forms a continuous vapor film. Cooling during this stage proceeds by film boiling and, if the part is at a sufficiently high temperature (i.e., steel), also by radiation. The second stage, *B*, is often denoted as the "vapor transport stage." This term is not really appropriate because during this stage there is a transition from

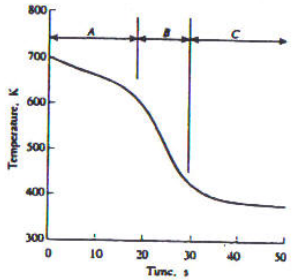


**Fig. 8.11** Cooling curve of a metal part quenched in water.

*Heated solid surfaces are subjected to *burnout*, unless the heating is reduced, because the operating point of the system will jump from point a to point b on the boiling curve.

partial nucleate boiling and unstable film boiling to entirely nucleate boiling. During stage C, referred to as the liquid cooling stage, there is less vapor formation, and eventually cooling occurs by only natural convection. Thus we see that as the metal cools from its initial elevated temperature to the fluid's temperature, it passes through all the regimes of the boiling curve (Fig. 8.10).

For these and other reasons, no comprehensive body of engineering correlations has evolved and been applied to quenching problems. Rather, most of the literature give some average values of $h$ which apply to specific cases.

For example, we can find the values of a parameter $H$, known as the *severity of quench*, and defined as $h/k$, which represent quenching practices for steel. Table 8.1 gives some typical values of $H$.

**Table 8.1** Severity of quench values and heat transfer coefficients for steel*

| Quench media | $H$-value, $m^{-1}$ | $h$, W $m^{-2}$ $K^{-1}$ |
|---|---|---|
| Oil, no agitation | 7.9 | 270 |
| Oil, moderate agitation | 13.8 | 480 |
| Oil, good agitation | 19.7 | 680 |
| Oil, violent agitation | 27.6 | 970 |
| Water, no agitation | 39.4 | 1400 |
| Water, strong agitation | 59.0 | 2000 |
| Brine, no agitation | 78.7 | 2700 |
| Brine, violent agitation | 196 | 6800 |

*Values of $H$ from M. A. Grossman, *Elements of Hardenability*, *ASM*, Cleveland, 1952; values of $h$ calculated using $k$ = 35 W $m^{-1}$ $K^{-1}$.

Data from this table should be applied only to conditions for which the values are derived. For example, $h$ can depend strongly on the temperature of the liquid media alone. The values shown above are for quenchants at room temperature. In addition, during quenching $h$ varies with the temperature of the solid itself. The values in Table 8.1 are derived specifically to predict the time to cool steel from its austenizing temperature to a temperature midway between the austenizing and original quench temperatures. Therefore all that we can say about the above $h$-values is that they are average and apply during cooling from about 1090 K to 690 K. It is left to the reader to comprehend the "political" terms—moderate agitation, good agitation, and violent agitation—given in Table 8.1.

For precipitation-hardenable aluminum alloys, an important step in their heat treatment is the cooling rate during quenching from the homogenization temperature. If the cooling rate is too low through a critical range of about 700 to 530 K, then precipitation occurs, and subsequent aging cannot be controlled. On the other hand, if the cooling rate during quenching is too great, then intolerable distortion in many parts occurs. In practice, therefore, heat treaters usually quench aluminum alloys in heated water to slow cooling and minimize distortion.

Brines, quenching oils, polymer solutions, and emulsions are used for quenching, in addition to water. Technological aspects, as well as heat transfer characteristics, of various quenchants are discussed in *Metals Handbook*[17] and in Sinha.[18] Usually, one of these

[17]*Metals Handbook*, Ninth edition, vol. 4, American Society for Metals, Metals Park, OH, 1981, pages 31-68 and 688-695.

[18]A. K. Sinha, *Ferrous Physical Metallurgy*, Butterworths Publ., Boston, MA, 1989, pages 442-460.



alternatives to water is selected when lower cooling rates are needed, except for brine, which causes a faster quench.

Figure 8.12 gives heat transfer coefficients measured for as-casts billets of copper immersed vertically in water. Figure 8.13 gives some values of $h$ for water/PAG (polyalkylene glycol) solutions based on experimentally measured cooling rates through the range 700-530 K. When solutions of PAG and water are used, $h$ is dependent on concentration. In these instances, an immiscible PAG-rich liquid phase forms at about 350 K (the exact temperature depends on the concentration). Thus, near the hot solid, the liquid separates into two immiscible liquid phases, and the surface becomes coated with the very viscous PAG-rich phase. Therefore, the rate of heat transfer is not controlled by a water vapor film whose thickness is dependent on the bulk water temperature to a large extent, but rather by the layer of the PAG-rich phase whose thickness and properties are presumably more predictable and not so much dependent on the bulk liquid temperature. Hence, more uniform cooling and reduction of distortion are achieved.

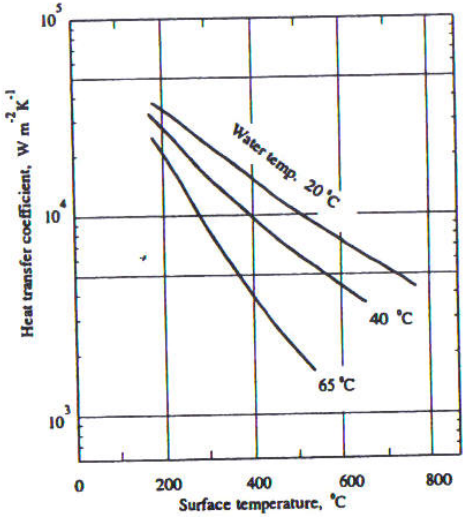


**Fig. 8.12** Heat transfer coefficients for immersion of copper billets in water. (From M. Bamberger and B. Prinz, *Mat. Sci. Tech.* 2, 410-415 (1986).)

Stolz[19] devised a numerical technique for obtaining heat transfer coefficients during quenching from measurements of interior temperatures of a solid sphere. By means of this technique heat transfer coefficients for quenching oils were evaluated as a function of the surface temperature of the solid. Figure 8.14 shows these data for oils designated as slow, intermediate, and fast. The figure also shows that between 1140 K and 895 K the heat transfer coefficients of all three types of oils are similar; over this range all three oils form a continuous vapor film on the solid's surface, and $h$ is only about 570 W $m^{-2}$ $K^{-1}$. From 645 K to 325 K, similar heat transfer coefficients are found for all three oils. The main differences among these oils lie in the regions where the heat transfer coefficients are greater

[19]G. Stolz, Jr., *J. Heat Transfer* **82**, 20-26 (1960).

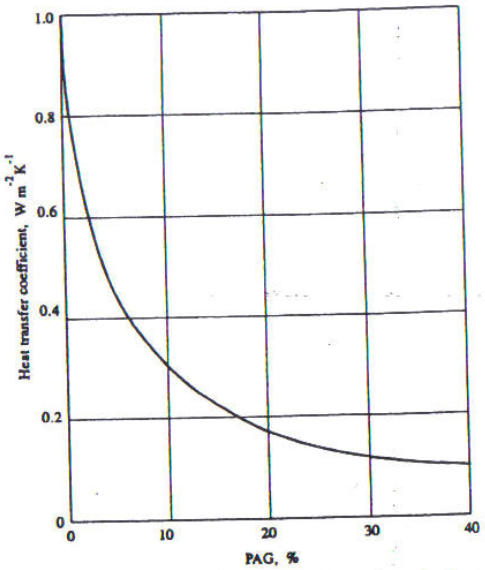


**Fig. 8.13** Heat transfer coefficients for cooling aluminum through the critical range of 700-530 K in water and water-polyalkylene glycol (PAG) solutions. (Reproduced by permission of Progressive Metallurgical Industries, Gardena, CA.)

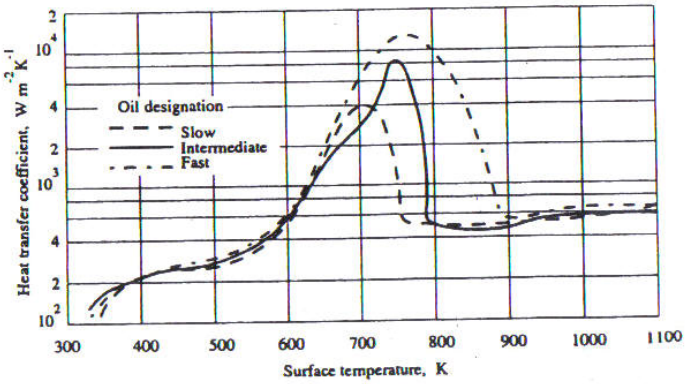


**Fig. 8.14** Heat transfer coefficients in quenching oils. (From G. Stolz, V. Paschkis, C. F. Bonilla, and G. Acevedo, *JISI* **193**, 116-123 (1959).)



than 570 W m$^{-2}$ K$^{-1}$, showing that the stable vapor film breaks down first (at a higher surface temperature) for the fast oil, and last for the slow oil.

The results for water and aqueous solutions of 1% NaOH and 5% NaOH are given in Fig. 8.15; all three solutions have a bulk temperature of 316 K. For these aqueous solutions, $h$ is initially between 1700 and 5100 W m$^{-2}$ K$^{-1}$. In a quench, these initial values of $h$ represent the rapid vaporization of water as the solid plunges into the water. This period is only a fraction of a second, after which $h$ drops to values indicative of the vapor film stage, but this is short-lived, especially for the 5% NaOH solution. The marked increase in heat transfer in the presence of NaOH over the range 1050 K-500 K is due to exploding salt crystals that make the vapor film unstable. All three solutions, however, reach the same peak value of $h$ at approximately 480 K.

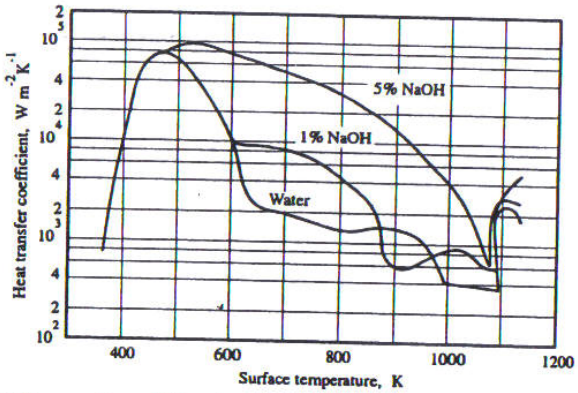


**Fig. 8.15** Heat transfer coefficients in aqueous quenching media. (From V. Paschkis and G. Stolz, Heat and Mass Flow Analyzer Laboratory, Columbia University, New York.)

In order to quench very long metal shapes, such as the strip from a hot strip mill or a continuously cast slab, we often use a multiplicity of water sprays. Figure 8.16 shows cooling data with a fan-type spray of water at 294 K which impinges on a hot horizontal surface from above. There is a sharp increase in the heat flux at about 900-750 K, which represents a transition from boiling with a vapor film to nucleate boiling.

When the vapor film is present during spray cooling, the rate of heat transfer depends on the degree to which the steam film can be broken down by the impinging droplets. With sprays, the droplets approaching the hot metal surface encounter the vapor film, and their success in penetrating this film depends on their kinetic energy. If the sprays are placed closer to the metal surface or the water velocity is increased, thereby increasing the droplets' kinetic energy, then the probability that the droplets will penetrate the film increases and so does the rate of heat removal.

With this in mind, it has been argued that a continuous stream of water, because of its high kinetic energy associated with its large mass, should penetrate the vapor film and bring about an increase in heat transfer rates.[20] For this reason, large nozzles in combination with low water pressure have been utilized to produce a falling stream, or jet, of water which does not break into droplets. For such a jet, an increase in the flow rate of water increases

[20] E. R. Morgan, T. E. Dancy, and M. Korchynsky, *J. Metals* **17**, No. 8, 829-831 (1965).

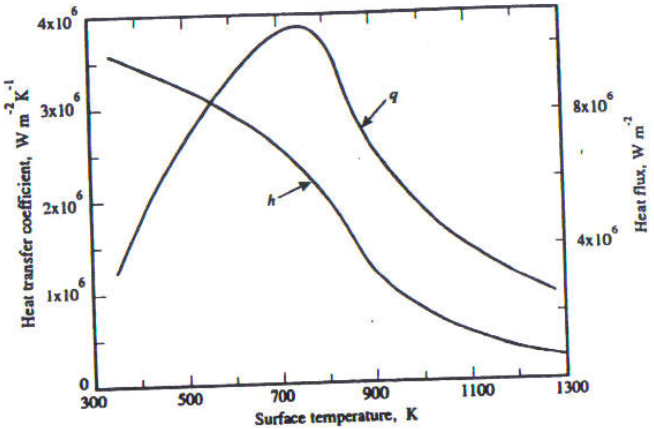


**Fig. 8.16** Heat flux and heat transfer coefficients for cooling a horizontal surface from above with a fan-type spray of water at 294 K. (Adapated from P. M. Auman, D. K. Griffiths, and D. R. Hill, *Iron Steel Engineer*, Sept., 1967.)

the rate of heat transfer up to a point. If the jet-flow rate passes a critical value, then the falling jet breaks up into less effective droplets, and the rate of heat transfer decreases.

In addition to water sprays, oil sprays have been used for quenching. It was found in a study,[21] that the cooling rate due to properly applied oil sprays was three to five times the cooling rate by immersing in oil in the conventional manner. Figure 8.17 shows some of these data.

Heat transfer coefficients for water spray cooling with slight overlapping of the spray cones are given in Fig. 8.18. Notice that results for immersion in water are also shown and that only the lines for the two highest spray intensities lie above the line for immersion in water.

## 8.5 HEAT TRANSFER COEFFICIENTS IN FLUIDIZED BEDS

Heat transfer in fluidized beds is of interest mainly because of a relatively new technology pertaining to combustion and gasification of solid fuels. Fluidized beds also are used extensively as dryers and chemical reactors. Here, however, we consider the fluidized bed as a possible medium for effecting the heating or cooling of immersed solids, as in heat treatment or quenching of metallic alloys.

Heat transfer between a fluidized bed and a solid surface immersed in the bed involves the convective heat transfer associated with the gas and the heat transfer associated with the contact between the fluidized particles and the immersed surface. The contact, itself, results in very little conduction and most of this heat transfer is associated with the complex

[21] N. V. Zimin, UDC 621.784.06, pages 854-858, Plenum Press, New York, 1968. Translated from *Metallovedenie i Termicheskaya Obrabotka Metallov*, No. 11, 62-68 (Nov., 1967).



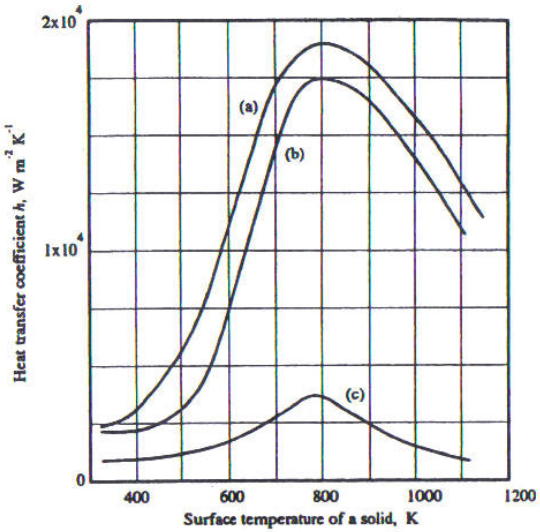


**Fig. 8.17** Heat transfer coefficients for oil-spray quenching and immersion in oil. (a) Very strong spray; flow rate > 0.70 $m^3 s^{-1} m^{-2}$. (b) Strong spray; flow rate = 0.60 $m^3 s^{-1} m^{-2}$. (c) Still oil. (From Zimin, *ibid.*)

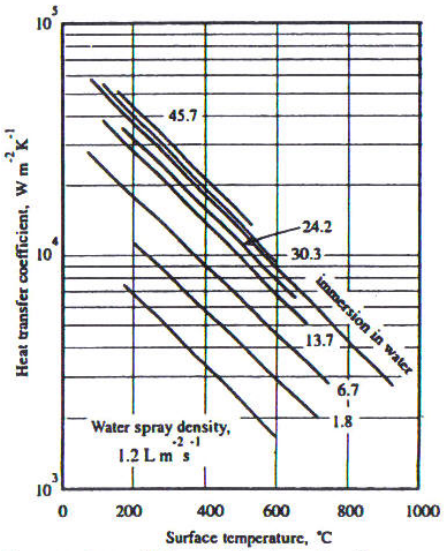


**Fig. 8.18** Heat transfer coefficient as function of surface temperature during spray cooling with various spray intensities. (From M. Bamberger and B. Prinz, *ibid.*)